

ORIGINAL ARTICLE

Magnetic resonance imaging of viral particle biodistribution *in vivo*

JK Rätty^{1,2}, T Liimatainen³, T Wirth^{1,2}, KJ Airene^{1,2}, TO Ihalainen⁴, T Huhtala⁵, E Hamerlynck³, M Vihinen-Ranta⁴, A Närvänen⁵, S Ylä-Herttua^{1,6,8} and JM Hakumäki^{3,7,8}

¹Department of Biotechnology and Molecular Medicine, University of Kuopio, Kuopio, Finland; ²Ark Therapeutics Oy, Neulaniementie 2L9, Kuopio, Finland; ³Cellular and Molecular Imaging Group, Department of Biomedical NMR, AI Virtanen Institute for Molecular Sciences, Kuopio, Finland; ⁴Department of Biological and Environmental Science, University of Jyväskylä, Jyväskylä, Finland; ⁵Department of Chemistry, University of Kuopio, Kuopio, Finland; ⁶Department of Medicine and Gene Therapy Unit, University of Kuopio, Kuopio, Finland and ⁷Department of Clinical Radiology, University of Kuopio, Kuopio, Finland

We describe here a technique for the visualization of viral vector delivery by magnetic resonance imaging (MRI) *in vivo*. By conjugating avidin-coated baculoviral vectors (Baavi) with biotinylated ultra-small superparamagnetic iron oxide particles (USPIO), we are able to produce vector-related MRI contrast in the choroid plexus cells of rat brain *in vivo* over a period of 14 days. Ten microlitres of 2.5×10^{10} PFU/ml nuclear-targeted LacZ-encoding Baavi with bUSPIO coating was injected into rat brain ventricles and visualized by MRI at 4.7 T. As baculoviruses exhibit restricted cell-type specificity in the rat brain, altered MRI contrast was detected in the choroid plexus of the injected ventricles. No specific signal

loss was detected when wild-type baculoviruses or intact biotinylated USPIO particles were injected into the lateral ventricles. Cryosectioned brains were stained for nuclear-targeted β -galactosidase gene expression, which was found to colocalize with MRI contrast. This study provides the first proof of principle for robust and non-invasive viral vector MRI by using avidin-displaying viruses *in vivo*. Considering the widespread use of MRI in current medical imaging, the approach is likely to provide numerous future applications in imaging of therapeutic gene transfer.

Gene Therapy advance online publication, 20 July 2006; doi:10.1038/sj.gt.3302828

Keywords: baculovirus; MRI; avidin; biodistribution; imaging

Introduction

Molecular medicine and gene transfer for therapeutic purposes are developing rapidly, and a pressing need for non-invasive, real-time *in vivo* detection of viral vectors has emerged. In recent years, nuclear magnetic resonance techniques and magnetic resonance spectroscopy have stepped into the limelight as a powerful imaging modality for detecting the effects of therapeutic gene therapy.^{1–3} In addition, magnetic resonance imaging (MRI) has been successfully employed to visualize gene expression *in vivo*,^{4,5} and more recently for detecting the presence of a ferritin marker gene after viral transduction in mouse brain *in vivo*.⁶

With these advances in mind, a robust, preferably non-invasive and widely applicable method for detecting the actual vectors would be highly desirable. Conventional imaging techniques for assessing viral biodistribution, such as immunohistochemistry or polymerase chain

reaction, are, albeit sensitive, highly laborious and lack the important non-invasive real-time option that would be required, especially for clinical work.

Vector imaging *in vivo* has remained a challenge, particularly by MRI. In gene therapy, it is essential to achieve targeted and efficient gene delivery. In order to achieve an optimal effect on the target tissue, gene delivery to non-target cells should remain as low as possible. Although efficient delivery of genes can be obtained by using non-viral vectors, such as polycationic dendrimers or liposomes, viral vectors are far more efficient in gene delivery to mammalian tissues *in vivo*.^{7,8} The biodistribution of viral vectors can vary greatly according to the properties of the surface proteins and their interaction with the cell surface. Viral targeting and pseudotyping have been used to modify the tropism and biodistribution of vectors used, most commonly with chemical or genetic modifications of the virus surface.^{9,10} Vector imaging and biodistribution studies *in vivo* would, therefore, not only be required for clinical applications, but also to examine the effects of such viral vector development. So far, viral vector imaging has only been achieved using whole-body nuclear imaging of rat¹¹ and rat brain.¹² Despite their sensitivity, the spatial resolution of nuclear imaging is poor (several millimeters), and the presence of ionizing radiation can be potentially harmful for cells. Also, the number of nuclear imaging scanners is clinically limited compared to MRI.

Correspondence: JK Rätty, Department of Biotechnology and Molecular Medicine, University of Kuopio, PO Box 1627, FIN 70211 Kuopio, Finland. E-mail: jani.ratty@uku.fi (JK Rätty); J Hakumäki or S Ylä-Herttua, AI Virtanen Institute for Molecular Sciences, University of Kuopio, PO Box 1627, FZN-70211, Kuopio, Finland. E-mails: Juhana.Hakumaki@uku.fi (JM Hakumäki); Seppo.Ylaherttua@uku.fi (S Ylä-Herttua)

⁸These authors contributed equally to the work

Received 1 March 2006; revised 12 June 2006; accepted 13 June 2006

The current study was designed to develop a technique to allow non-invasive imaging of baculoviral biodistribution *in vivo* by MRI. Baculoviruses have been shown to be effective gene transfer vectors in vertebrate cells.^{13,14} The recently developed, avidin-displaying baculovirus Baavi¹⁵ enables coating of the virus with a multitude of biotinylated molecules, and thus results in a versatile platform for labeling and to study and influence baculovirus-mediated gene delivery. In this study, we used biotinylated ultra-small superparamagnetic iron oxide particles (USPIO) to visualize the accumulation of avidin-displaying viruses in rat brain *in vivo*. Similar iron oxide nanoparticles have been applied to track iron-labeled stem cells *in vivo*^{16,17} and the detection of apoptosis *in vivo*,¹⁸ as well as for receptor-mediated magnetic labeling of cancer cells.¹⁹ In this study, we describe a proof-of-principle method for efficient non-invasive visualization of viral vector targeting *in vivo* – a gene transfer technique that has not so far been utilized within the potential applications of *in vivo* MRI.

Results

In order to obtain information about the binding of nanoparticles to the virus (Figure 1a), atomic force microscopy (AFM) was used. The results confirm that nanoparticles of the estimated size are bound to the virus surface with an average of 1–2 virions per particle (Figure 1b). bUSPIO were detected in the size range of 42 ± 7 nm in conjunction with viral particles (ranging 200–300 and 24–27 nm in length and width, respectively). The results are in general agreement with our previous results using gold and larger iron oxide particles.¹⁵ Transduction assays in HepG2 cell lines show that bUSPIO coating of the avidin-displaying baculovirus (Baavi) increased both transduction efficiency (Figure 2a) and transgene expression level (Figure 2b).

When avidin-displaying viruses were conjugated with bUSPIO before injection, viruses could be detected in the ipsilateral ventricle of rat brain, even with the earliest

technically obtainable time point (2 h after injection). The animals underwent MRI scans at 4.7 T at time points of 2 h and 1, 3, 6 and 14 days after the injection. Using gradient echo contrast, which renders tissue more susceptible to the field-dephasing effects of iron oxide, the signal could be further enhanced but at the cost of anatomic reference points (Figure 3a). Using spin-echo contrast, however, sufficient contrast effects could be detected with less blooming effect and better anatomical acuity (Figure 3b). This signal loss could be visualized from the ipsilateral ventricle (Figure 3c) of the rat brain with avidin-displaying viruses (Figure 4a). We then

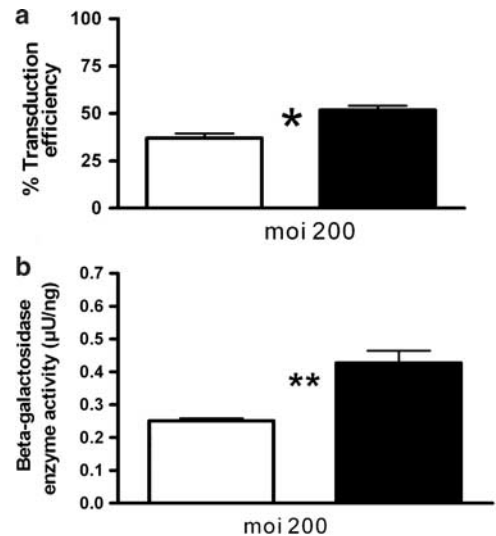


Figure 2 Comparison of transduction ability of non-coated (white bars) and bUSPIO-coated Baavi (black bars) in HepG2 cells at MOI 200. Transduction efficiency was measured by counting percentage of positive blue cells after X-gal staining (a) and expression levels of β -galactosidase were measured quantitatively by luminescence assay from lysed and normalized cell population (b). Results are shown as average \pm s.e.m.; $n=4-6$; * $P < 0.05$, ** $P < 0.01$; Student's unpaired *t*-test.

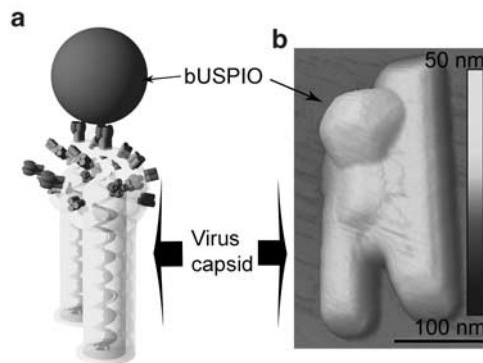


Figure 1 Presentation of bUSPIO-conjugated avidin-displaying baculovirus (Baavi). The construct structure together with virus and 50 nm bUSPIO is described in the schematic figure (a). bUSPIO attachment to viral particles was confirmed by AFM (b). In-plane scale bar is shown at the bottom; out-of-plane scale (height) is demonstrated by sliding color scale.

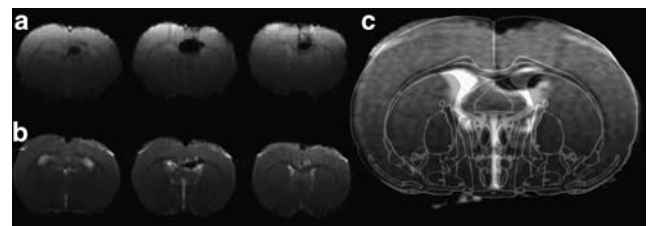


Figure 3 MRI of intraventricular bUSPIO+Baavi delivery. Representative sequential transverse T_2^* -weighted gradient echo MRI images are (a) compared to sequential adiabatic T_2 -weighted spin-echo images (b) 2 h after bUSPIO-coated Baavi injection. Bright represents high signal intensity (such as cerebrospinal fluid in ventricles), and dark areas low signal intensity owing to the presence of contrast agent. As can be seen, remarkable signal loss is detectable in T_2^* -weighted MRI images (a), showing that gradient echo imaging provides improved sensitivity. However, sensitivity appears sufficient, and anatomical features are better preserved and delineated in (b). A superimposed anatomical reference map together with spin echo image (c) of rat brain after Baavi+bUSPIO is also shown from one animal. In this composite, ventricles are of high signal intensity (white) and brain regions are delineated by gray lines.

examined whether nonspecific binding of bUSPIO could cause this signal loss and found that either 2 h after the injection or 1 day later, an equal amount of plain bUSPIO did not generate similar contrast (Figure 4b) to that observed in animals injected with bUSPIO-conjugated Baavi. Also, the MRI imaging did not have any effect on the transduction pattern of bUSPIO-labeled Baavi (data not shown).

To verify that the contrast was generated by viral particles carrying iron oxides, we examined its correlation to iron detectable in rat brain. For this purpose, we examined cryosectioned brain slices for iron with the Prussian blue method. However, as the total amount of the accumulated iron in rat brain was expected to be quite low, we used diaminobenzene (DAB) enhancement for better visualization. Negative controls showed no detectable deposition of iron in choroid plexus cells (Figure 5a). When bUSPIO-coated baculoviruses were injected directly into brain parenchyma to serve as an internal positive control, significant iron-positive staining could be observed (Figure 5b) from consecutive sections. Upon examination of rat brains injected with bUSPIO-coated Baavi, we found consistent staining of cuboid epithelial cells of the choroid plexus cells in tissue sections from the ipsilateral side (Figure 5c), whereas the rest of the brain remained unstained. This staining was in good agreement with the MRI data. No significant staining could be observed on the contralateral side (data not shown).

After successfully demonstrating that Baavi could be detected by MRI *in vivo*, we wanted to verify the true utility of the technique by demonstrating that the coating of the virus vector had not affected its capacity to transduce choroid plexus cells. To achieve this, we assessed the expression of the nuclear-targeted *LacZ* transgene with β -galactosidase staining from cryosectioned rat brains (Figure 6). We showed previously that baculovirus exhibits strong tropism towards cuboid epithelial cells of choroid plexus in the ventricles.¹⁴ Wild-type *LacZ* baculovirus with the same expression cassette resulted in gene expression detected almost exclusively in choroid plexus cells (Figure 6a). Interestingly, as compared to the non-coated Baavi (Figure 6b), the expression pattern was somewhat wider with bUSPIO coating, and extensive expression was seen in choroid plexus cells (Figure 6c). Expression of the bUSPIO-coated Baavi was comparable to wild-type *LacZ* baculovirus,

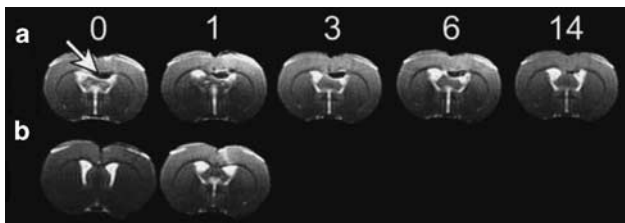


Figure 4 Adiabatic T_2 -weighted spin-echo magnetic resonance images. Rat brain is imaged 0–14 days after injection of bUSPIO-coated Baavi (a), and plain bUSPIO without virus (b). bUSPIO-coated Baavi injected into the lateral ventricle causes a long-lasting ipsilateral signal loss corresponding to choroid plexus uptake as confirmed by histology, whereas no contrast changes are detectable in animals that received an intraventricular injection of pure contrast agent (bUSPIO) only.

with large numbers of positively stained cells in the choroid plexus. A few positive cells were also detected on the contralateral side in some brain slices (data not shown). However, as the number of such cells was extremely low, contribution to the MRI contrast was expected to be negligible.

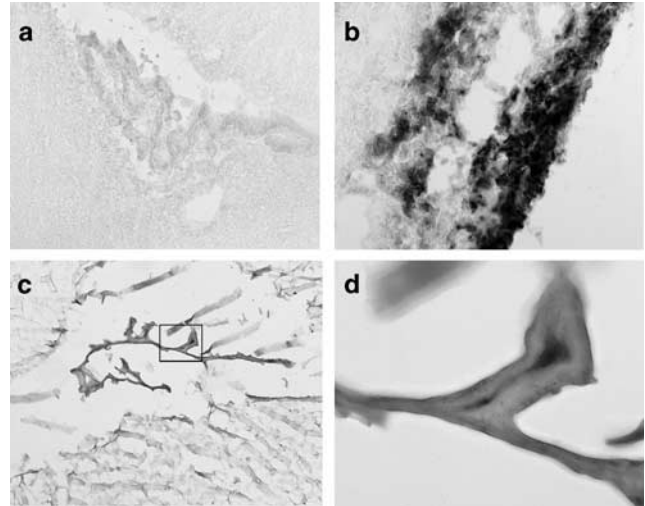


Figure 5 DAB-enhanced Prussian blue iron stainings of cryosectioned rat brain slices showing choroid plexus cells 5 days after injections. No staining (a) is observed in rat injected with bUSPIO only (negative control), whereas bUSPIO+Baavi injected directly into brain parenchyma (b) showed a highly positive signal for trapped iron (positive control). Positive ipsilateral staining of choroid plexus cells could be observed after bUSPIO+Baavi injection into lateral ventricle (c), with a $\times 400$ original magnification of the boxed area showing positive staining inside the cells (d). Images a–c are $\times 100$ original magnification.

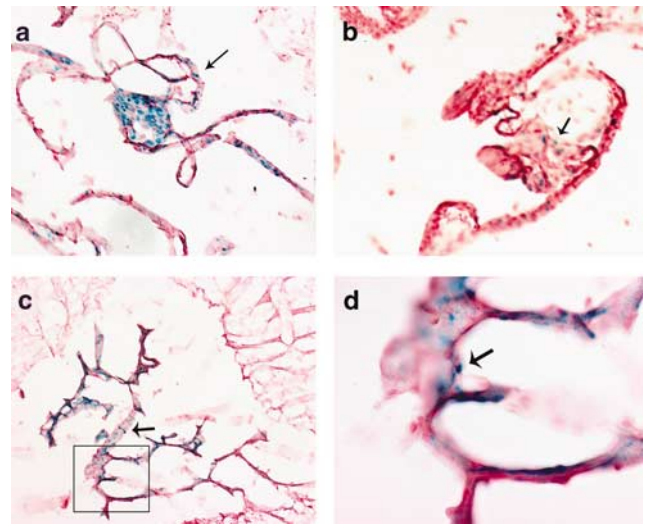


Figure 6 β -Galactosidase stainings from cryosectioned rat brain slices with Mayer's Carmalum counterstain showing choroid plexus cells of ipsilateral ventricle 5 days after the injection. *LacZ* marker gene expression can be seen as blue staining (indicated with arrow) in choroid plexus cells with (a) wild-type baculovirus with *LacZ* marker gene, (b) Baavi with *lacZ* alone and (c) bUSPIO+Baavi with *lacZ*. $\times 400$ original magnification of boxed area of (c) is also shown (d). Images a–c are $\times 100$ original magnification.

Our data therefore indicate that on the basis of the β -galactosidase expression and positive iron staining, both baculoviruses and bUSPIO particles were colocalized to the choroid plexus cells, and could thus be accurately visualized by MRI.

To address whether the techniques used here exposed the cells to unknown toxic effects, we used a standard methyl thiazole tetrazolium (MTT) assay *in vitro*, and found no indication of increased cytotoxicity with non-coated or bUSPIO-coated Baavi (data not shown). This finding is in agreement with the previous work¹⁵ and results from *in vivo* MRI study.²⁰ Furthermore, neither apparent gross cytotoxic effects nor hydrocephalus was associated with the injection of Baavi and bUSPIO *in vivo* on histology sections or MRI.

Discussion

In this study, we demonstrate a proof-of-principle for MRI detection of viral biodistribution *in vivo*. By coating avidin-displaying baculoviruses with bUSPIO, we were able to use MRI for visualizing viral biodistribution in rat brain *in vivo* during different time points.

As AFM produces accurate dimensional data after non-destructive measurement and is less vulnerable to imaging artifacts than electron microscopy,²¹ we used AFM to determine the size and composition of bUSPIO/Baavi complexes. We observed that keeping the viral particles highly saturated (100:1) with multibiotinylated USPIO during the overnight coating limited the formation of crosslinked aggregates, resulting in small-sized iron-virus complexes with a median of 1–2 virus per bUSPIO. We conclude that these factors together improved bUSPIO-Baavi diffusion to CSF *in vivo*.

To compare the transduction performance of the bUSPIO-coated and non-coated Baavi *in vitro*, we evaluated both the transduction efficiency and the expression level of the β -galactosidase marker protein. bUSPIO coating increased both transduction efficiency and expression level of the transgene, which is in agreement with the described transduction mechanism of iron particle complexes.²²

After the intraventricular injection into the rat brain, we found a specific loss of MRI signal on the injected side of the rat brain ventricle, consistent with iron oxide loading, which remained detectable for 2 weeks. Baculoviruses are known to exhibit strong tropism towards choroid plexus cells,¹⁴ and the accumulation of iron in these cells helps to explain the MRI contrast changes in the corresponding areas of the rat brain. Even though the choroid plexus cells are known to have extensive endocytotic traffic,²³ the contrast changes could not be explained by passive endocytosis of the bUSPIO particles, as no MRI signal changes could be detected in animals receiving an equal amount of iron in a plain bUSPIO suspension. The slight blooming effect observable in spin echo images causes the region of enhanced contrast (i.e. signal loss) to be a few millimeters larger than the area actually confirmed by histochemical methods.²⁴

The loss of the MRI signal during time studied here may be explained by choroid plexus cell turnover or even cell proliferation as a response to injury.²⁵ After intracerebral administration, USPIO particles have been

observed to accumulate in cervical lymph nodes via CSF efflux,²⁴ which agrees with our previous findings of baculovirus systemic escape to ectopic tissues.¹⁴ These observations could explain the fate of non-uptaken bUSPIO and bUSPIO-Baavi complexes that are not taken up.

Neither spin nor gradient echo imaging results in signal loss after ventricular injection of bUSPIO or Baavi alone. Owing to anesthesia, the first technically obtainable time point was 2 h. The iron administered (500 ng) in these control studies diffuses to the rat ventricular system ($\sim 300 \mu\text{l}$) and reaches a maximal concentration of only $1.7 \text{ ng}/\mu\text{l}$. Moreover, as CSF clearance is reportedly rapid²⁶ with 1 h turnover in rats,²⁷ after 2 h (the/any) unbound bUSPIO or non-endocytosed bUSPIO-Baavi particles are likely to have diluted and escaped from CSF as reported previously.²⁴ The transduction efficiency of the bUSPIO-labeled Baavi in choroid plexus cells *in vivo* is in line with our previous findings¹⁴ of baculovirus without avidin.

The relationship of the iron originated signal loss to the biodistribution of the baculovirus was confirmed by two independent methods, firstly by DAB-enhanced Prussian blue staining for iron and secondly by β -galactosidase staining for the viral LacZ transgene expression. Both methods resulted in staining of the cuboid epithelial cells of the choroid plexus. As the CSF flow originates from the lateral ventricles and passes through the third and fourth ventricles to the superior sagittal sinus via the subarachnoid space,²⁸ the liquid dynamics are likely to prevent the diffusion of bUSPIO-virus particles from the injected ipsilateral ventricle to the contralateral ventricle. This hypothesis was confirmed by our unilateral MRI data, β -galactosidase staining resulting in only a few positive cells and by the less sensitive Prussian blue staining, which did not result in staining on the contralateral side. Some positive cells were also seen in the brain parenchyma as we have observed occasionally also with non-coated Baavi after ventricular injection.

The data confirm the colocalization of bUSPIO with Baavi and moreover indicate that Baavi can deliver cargo to choroid plexus cells. As human choroid plexus cells produce 500 ml CSF per day and are reported to be involved in various medical conditions²³ and even in brain regeneration,²⁵ the possibility of affecting the central nervous system by gene therapy via the CSF would be intriguing. As gene therapy continues to evolve towards clinical applications,²⁹ the need to develop more efficient vectors has become evident. A deeper understanding of the molecular aspects of the vector delivery and distribution can only be achieved by the development of new *in vivo* imaging methods for non-invasive, real-time detection of the actual viral vectors. The non-invasive detection of marker genes⁶ is an elegant indicator of successful gene transfer, essentially serving as a surrogate marker for the vector. However, imaging of transgene expression is limited to the detection of permissive cells only, whereas possible entrapment of viral vectors to non-permissive cells could be overlooked.

With these findings, we have now reached a point where all three major phases, namely delivery, expression and outcome, of therapeutic gene transfer can be visualized by MRI. This could decrease the time and

effort needed to examine the effect of targeting molecules on virus biodistribution. More work is still needed to develop MRI-based quantification of viral biodistribution to the level of radionuclide imaging, however. Nuclear imaging techniques are inherently quantitative, and can be several magnitudes more sensitive than MRI, which is a clear advantage in whole-body biodistribution studies. Unlike iron oxide nanoparticles, isotope labels are small and labeling strategies are more straightforward. However with MRI, animals are not subjected to radiation, and the spatial resolution is far superior to isotope techniques (which, at best, are in the millimeter range). While this study was conducted using avidin-displaying baculovirus, the proof-of-principle concept using an avidin–biotin vector platform could be extended to other viruses,^{30,31} thus widening the MRI applications available for use in gene therapy.

Materials and methods

Biotinylation of nanoparticles

USPIO particles (50 nm; PMC-50, Fe₃O₄ Kisker GMBH, Steinfurt, Germany) were coated with *d*-biotin (Sigma-Aldrich, St Louis, MO, USA) by using *O*-benzotriazole-*N,N,N',N'*-tetramethyl-uronium-hexafluorophosphate (HBTU, GL Biochem Ltd, Shanghai, China) as a coupling reagent. Ten milligrams of USPIO particles (5 mg/ml in water) was mixed with 80 mmol of HBTU dissolved in 1.5 ml of dimethylformamide (DMF) and divided into two vials. Then 150 mmol of biotin dissolved in 2 ml of DMF and 2 ml of pure DMF were added to the vials. Finally, 20 μ l of diisopropyl ethanolamine (DIPEA, Fluka, Steinheim, Germany) was added to both vials and the vials were mixed in an end-over-end mixer for 2 h at room temperature (RT). After incubation, biotinylated and control particles were transferred to dialysis cassettes (MWCO 10000, Pierce, Rockford, IL, USA) and dialysed against phosphate-buffered saline (PBS) pH 7.4 overnight at RT. The particles were concentrated to 5 mg/ml in PBS by using Amicon Ultra Centrifugal Filter Device MWCO 30000 (Millipore, Billerica, MA, USA). The biotinylation of the USPIO particles was verified by using a pull-down test with streptavidin Sepharose (17-5113-01, Amersham Biosciences AB, Uppsala, Sweden) suspension. The particles were mixed with Sepharose suspension with and without free biotin and after 5 min incubation the Sepharose was centrifuged down. The color of the supernatants and Sepharose of the biotinylated and control particles were monitored by eye and the supernatants was further measured with spectrophotometer at 405 nm.

Coating viruses with bUSPIO

Avidin-displaying baculovirus¹⁵ (2.5×10^{10} infective particles/ml) was mixed with biotinylated 50 nm superparamagnetic nanoparticles with a ratio of ~ 100 spheres per infective virus particle (in 1:100 spheres/virus volume) and allowed to incubate overnight at +4°C.

MTT assay

Cytotoxicity of Baavi or bUSPIO-coated Baavi was determined by CellTiter 96 Aqueous One Solution Cell Proliferation Assay (Promega, Madison, WI, USA) according to the manufacturer's instructions. The mea-

surements were carried out with a minimum of five replicates. Absorbance was measured at 492 nm. Survival percentages were calculated by comparison with the absorbances of the no virus wells or no butyrate wells (100% survival).

Transduction efficiency

HepG2 cells were seeded at 20 000 cells per 12-well plates in their recommended medium. After 24 h, the medium was removed and fresh complete medium containing virus dilutions was added. After 24 h incubation, cells were fixed with 1.25% glutaraldehyde and stained with X-gal to visualize β -galactosidase-expressing cells and blue cells were counted.

β -Galactosidase enzyme assay

Luminescent β -galactosidase enzyme assay (Clontech, BD Biosciences, Mountain View, CA, USA) was used to analyze the amount of enzyme expressed in the transduced cells according to the manufacturer's instructions. The luminescence was measured with black luminometer 96-well plates (Black Isoplate TC Wallac, Turku, Finland) and Victor² luminometer (Wallac, Turku). Coomassie Plus protein assay (Bio-Rad, Hercules, CA, USA) was used to equalize the protein amounts from lysed cell samples according to the manufacturer's instructions.

AFM

For AFM imaging, nanoparticles and viruses were mixed 1:1 and incubated for 1 h at RT. After incubation, 20 μ l of the mixture was placed on freshly cleaved mica (SPI Supplies, West Chester, PA, USA) and the sample was dried in a desiccator for 1 h. Before the AFM imaging, samples were washed with distilled water and carefully dried using a N₂ stream. Dry samples were imaged with a Dimension 3100 Atomic Force Microscope with Nanoscope IV controller (Veeco Instruments, Santa Barbara, CA, USA). Imaging was conducted in tapping mode using RTESP tips (Veeco Instruments, Rochester, NY, USA) and a scanning speed of 1–2 Hz. NANO-SCOPE 6.11 software (Veeco Instruments) was used for the analyses.

Stereotactic injections to rat ventricles

Female inbred BDIX rats (200–250 g) were anesthetized intraperitoneally with a solution (0.150 ml/100 g) containing fentanyl fluanisone (Janssen-Cilag, Hypnorm, Buckinghamshire, UK) and midazolam (Roche, Dormicum, Basel, Switzerland) and placed into stereotactic apparatus (Kopf Instruments, Tujunga, CA, USA). A total volume of 10 μ l of the virus and bUSPIO solution in PBS/0.1% sucrose was injected using a Hamilton syringe with a 27-gauge needle into the right ventricle (coordinates: 1.0 mm caudal to bregma, 1.5 mm right to sutura sagittalis, and depth of 3.5 mm). The total amount of iron administered was 500 ng with 2.5×10^8 infective baculoviral particles per animal. Rats were killed at different time points, perfused with PBS intracardially and fixed in X-gal fix for 30 min. The brains were rinsed for 2 h in PBS, after which they were embedded in OCT for cryosectioning.

MRI

The Baavi animals underwent MR imaging 1–2 h after injection, with additional scans 1, 3, 6 ($n = 7$) and 14 days ($n = 2$) later. A control group received bUSPIO only and was imaged 2 h and 1 day after the injection ($n = 3$). All MRI experiments were performed in a 4.7 T magnet (Magnex, Abington, Oxfordshire, UK) interfaced to Varian Unity ANOVA console (Varian Inc., Palo Alto, CA, USA). A quadrature half-volume coil (diameter 20 mm) was used (HF Imaging LLC, Minneapolis, MN, USA) in transmit/receive mode. Transverse multi-slice gradient echo images (echo time (TE) = 10–20 ms, repetition time (TR) = 0.32 s, number of slices (NS) = 11, field of view (FOV) = 3.5×3.5 cm², number of points in echo (NP) = 512 and number of phase encoding steps (NV = 128)) were obtained in addition to localized adiabatic spin echo multi-slice images (TE = 75 ms, TR = 2 s, NS = 11, FOV = 3.5×3.5 cm², NP = 512 and NV = 128). Animals were anesthetized with 1% halothane in 74%:25% N₂O:O₂, respectively, and fastened to a stereotactic holder with ear pins and mouth bar. Animal core temperature was maintained close to 37°C using a water-heated pad. Image reconstruction and analyses were performed using Matlab (Mathworks, Natick, MA, USA) routines.

β -Galactosidase staining

Cryosectioned rat brain sections (12 μ m) were washed 2×5 min with PBS and incubated overnight with X-gal staining solution (1 mg/ml 5-bromo-4-chloro-3-indolyl-beta-D-galactopyranoside in *N,N*-dimethylformamide added to 5 mM K₃Fe(CN)₆, 5 mM K₄Fe(CN)₆ and 2 mM MgCl₂) at +37°C. Slides were rinsed with PBS and counterstained with Mayer's Carmalum, fixed with increasing concentrations of ethanol and mounted with Permount.

DAB enhanced iron detection

Cryosectioned brain slices were washed with PBS and incubated for 1 h with Prussian blue reagent (fresh 1:1 solution of 2% HCl with 2% K₄Fe(CN)₆), and then washed 2×5 min in PBS and incubated for 20 min with 1:10 solution of DAB. After this slices were washed with PBS and fixed with increasing concentrations of ethanol and mounted with Permount.

Statistical analyses

GraphPad Prism (GraphPad Software Inc., San Diego, CA, USA) and Student's unpaired *t*-test were used for statistical analyses.

Acknowledgements

We thank the Finnish Academy (JH, SY), the Sigrid Juselius Foundation (JH, SY), Instrumentarium Science Foundation (JH, TL), Onion Science Foundation (TL) and Ark Therapeutics Ltd (JR, TW, KA) for support.

References

- Hakumaki JM, Poptani H, Sandmair AM, Yla-Herttuala S, Kauppinen RA. 1H MRS detects polyunsaturated fatty acid accumulation during gene therapy of glioma: implications for the *in vivo* detection of apoptosis. *Nat Med* 1999; 5: 1323–1327.
- Maron A, Gustin T, Le Roux A, Mottet I, Dedieu JF, Brion JP *et al*. Gene therapy of rat C6 glioma using adenovirus-mediated transfer of the herpes simplex virus thymidine kinase gene: long-term follow-up by magnetic resonance imaging. *Gene Therapy* 1996; 3: 315–322.
- Evelhoch JL, Gillies RJ, Karczmar GS, Koutcher JA, Maxwell RJ, Nalcioglu O *et al*. Applications of magnetic resonance in model systems: cancer therapeutics. *Neoplasia* 2000; 2: 152–165.
- Weissleder R, Moore A, Mahmood U, Bhorade R, Benveniste H, Chiocca EA *et al*. *In vivo* magnetic resonance imaging of transgene expression. *Nat Med* 2000; 6: 351–355.
- Stegman LD, Rehemtulla A, Beattie B, Kievit E, Lawrence TS, Blasberg RG *et al*. Noninvasive quantitation of cytosine deaminase transgene expression in human tumor xenografts with *in vivo* magnetic resonance spectroscopy. *Proc Natl Acad Sci USA* 1999; 96: 9821–9826.
- Genove G, DeMarco U, Xu H, Goins WF, Ahrens ET. A new transgene reporter for *in vivo* magnetic resonance imaging. *Nat Med* 2005; 11: 450–454.
- Glover DJ, Lipps HJ, Jans DA. Towards safe, non-viral therapeutic gene expression in humans. *Nat Rev Genet* 2005; 6: 299–310.
- Kootstra NA, Verma IM. Gene therapy with viral vectors. *Annu Rev Pharmacol Toxicol* 2003; 43: 413–439.
- Turunen MP, Puhakka HL, Koponen JK, Hiltunen MO, Rutanen J, Leppanen O *et al*. Peptide-retargeted adenovirus encoding a tissue inhibitor of metalloproteinase-1 decreases restenosis after intravascular gene transfer. *Mol Ther* 2002; 6: 306–312.
- Volpers C, Thirion C, Biermann V, Hussmann S, Kewes H, Dunant P *et al*. Antibody-mediated targeting of an adenovirus vector modified to contain a synthetic immunoglobulin g-binding domain in the capsid. *J Virol* 2003; 77: 2093–2104.
- Schellingerhout D, Bogdanov Jr A, Marecos E, Spear M, Breakefield X, Weissleder R *et al*. Mapping the *in vivo* distribution of herpes simplex virions. *Hum Gene Ther* 1998; 9: 1543–1549.
- Schellingerhout D, Rainov NG, Breakefield XO, Weissleder R. Quantitation of HSV mass distribution in a rodent brain tumor model. *Gene Therapy* 2000; 7: 1648–1655.
- Airenne KJ, Hiltunen MO, Turunen MP, Turunen AM, Laitinen OH, Kulomaa MS *et al*. Baculovirus-mediated periaxillary gene transfer to rabbit carotid artery. *Gene Therapy* 2000; 7: 1499–1504.
- Lehtolainen P, Tyynela K, Kannasto J, Airenne KJ, Yla-Herttuala S. Baculoviruses exhibit restricted cell type specificity in rat brain: a comparison of baculovirus- and adenovirus-mediated intracerebral gene transfer *in vivo*. *Gene Therapy* 2002; 9: 1693–1699.
- Raty JK, Airenne KJ, Marttila AT, Marjomaki V, Hytonen VP, Lehtolainen P *et al*. Enhanced gene delivery by avidin-displaying baculovirus. *Mol Ther* 2004; 9: 282–291.
- Bulte JW, Duncan ID, Frank JA. *In vivo* magnetic resonance tracking of magnetically labeled cells after transplantation. *J Cereb Blood Flow Metab* 2002; 22: 899–907.
- Bai H, Morishita R, Kida I, Yamakawa T, Zhang W, Aoki M *et al*. Inhibition of intimal hyperplasia after vein grafting by *in vivo* transfer of human senescent cell-derived inhibitor-1 gene. *Gene Therapy* 1998; 5: 761–769.
- Zhao M, Beauregard DA, Loizou L, Davletov B, Brindle KM. Non-invasive detection of apoptosis using magnetic resonance imaging and a targeted contrast agent. *Nat Med* 2001; 7: 1241–1244.
- Artemov D, Mori N, Okollie B, Bhujwala ZM. MR molecular imaging of the Her-2/neu receptor in breast cancer cells using targeted iron oxide nanoparticles. *Magn Reson Med* 2003; 49: 403–408.

1 Hakumaki JM, Poptani H, Sandmair AM, Yla-Herttuala S, Kauppinen RA. 1H MRS detects polyunsaturated fatty acid

- 20 Muldoon LL, Sandor M, Pinkston KE, Neuwelt EA. Imaging, distribution, and toxicity of superparamagnetic iron oxide magnetic resonance nanoparticles in the rat brain and intracerebral tumor. *Neurosurgery* 2005; **57**: 785–796.
- 21 Horber JK, Miles MJ. Scanning probe evolution in biology. *Science* 2003; **302**: 1002–1005.
- 22 Huth S, Lausier J, Gersting SW, Rudolph C, Plank C, Welsch U *et al*. Insights into the mechanism of magnetofection using PEI-based magnetofectins for gene transfer. *J Gene Med* 2004; **6**: 923–936.
- 23 Emerich DF, Skinner SJ, Borlongan CV, Vasconcellos AV, Thanos CG. The choroid plexus in the rise, fall and repair of the brain. *BioEssays* 2005; **27**: 262–274.
- 24 Muldoon LL, Varallyay P, Kraemer DF, Kiwic G, Pinkston K, Walker-Rosenfeld SL *et al*. Trafficking of superparamagnetic iron oxide particles (Combidex) from brain to lymph nodes in the rat. *Neuropathol Appl Neurobiol* 2004; **30**: 70–79.
- 25 Li Y, Chen J, Chopp M. Cell proliferation and differentiation from ependymal, subependymal and choroid plexus cells in response to stroke in rats. *J Neurol Sci* 2002; **193**: 137–146.
- 26 Nagaraja TN, Patel P, Gorski M, Gorevic PD, Patlak CS, Fenstermacher JD. In normal rat, intraventricularly administered insulin-like growth factor-1 is rapidly cleared from CSF with limited distribution into brain. *Cerebrospinal Fluid Res* 2005; **2**: 5.
- 27 Davson H, Segal MB. *Physiology of the CSF and Blood–Brain Barriers*. CRC Press: Boca Raton, FL, 1996.
- 28 Knopf PM, Cserr HF, Nolan SC, Wu TY, Harling-Berg CJ. Physiology and immunology of lymphatic drainage of interstitial and cerebrospinal fluid from the brain. *Neuropathol Appl Neurobiol* 1995; **21**: 175–180.
- 29 Pulkkanen KJ, Sallinen H, Tyynela K, Yla-Herttuala S. Cancer gene therapy – current status in the clinics. *Gene Ther Regul* 2004; **3**: 219–274.
- 30 Puro B, Staveley-O’Carroll K. Targeting of vaccinia virus using biotin–avidin viral coating and biotinylated antibodies. *J Surg Res* 2005; **123**: 49–54.
- 31 Parrott MB, Adams KE, Mercier GT, Mok H, Campos SK, Barry MA. Metabolically biotinylated adenovirus for cell targeting, ligand screening, and vector purification. *Mol Ther* 2003; **8**: 688–700.